Tuning from π,π^* to Charge-Transfer Excited States in Styryl-Substituted Terthiophenes: An Ultrafast and Steady-State Emission Study

Tracey M. Clarke,[†] Keith C. Gordon,*[,†] Wai Ming Kwok,[‡] David Lee Phillips,[‡] and David L. Officer[§]

Department of Chemistry and MacDiarmid Institute for Advanced Materials and Nanotechnology, University of Otago, PO Box 56, Dunedin, New Zealand, Department of Chemistry, The University of Hong Kong, Pokfulam Road, Hong Kong S. A. R., P. R. China, and Nanomaterials Research Centre and MacDiarmid Institute for Advanced Materials and Nanotechnology, Massey University, Private Bag 11222, Palmerston North, New Zealand

Received: January 3, 2006; In Final Form: April 13, 2006

The steady-state and transient emission properties of unsubstituted terthiophene and a series of 3′-[*E*-2-(4-R-phenyl)ethenyl]-2,2′:5′,2″-terthiophenes (where R = H, MeO, NH_2, CN, NMe_2, NO_2) have been examined. The R = NO_2 compound is nonemissive at room temperature in all solvents but cyclohexane. All of the other compounds show measurable steady-state emission in a variety of solvents. The behavior of these spectra may be split into two groups. The first group, those substituted compounds with R = CN, NH_2 and NMe_2, show solvatochromic behavior, where their Lippert−Mataga plots suggest changes in dipole upon photoexcitation ranging from 12.5 to 16.0 D. For the second group, where R = H and MeO (and unsubstituted terthiophene as well), the Lippert−Mataga plots indicate dipole moment changes ranging from 0 to 7.9 D. The difference in behavior between the two groups of emissive compounds can be attributed to a charge-transfer character of the emitting state in the first group. This conclusion is supported by density functional theory calculations, which show that the frontier MOs in the group one compounds are spatially separated whereas those of group two have frontier MOs that are delocalized over both the styryl and terthiophene moieties. Picosecond time-resolved fluorescence spectroscopy reveals that unsubstituted terthiophene has the shortest emission lifetime of 140 ps in acetonitrile. For the styryl substituted terthiophenes, the lifetimes are much longer and range from 320 to 670 ps for R = CN and NMe_2 respectively, a result that can be explained in terms of a smaller rate of intersystem crossing in these compounds.

Introduction

Oligothiophenes have proven to be useful components in plastic electronic devices[1] such as organic light emitting diodes,[2] field effect transistors[3] and photovoltaic cells.[4] However, the charge conduction mechanism in these devices still requires elucidation. Advancing the understanding of organic conductors may allow a more rational design of these molecules, thereby enhancing the efficiency of the resultant devices. The creation and behavior of excitons is of particular importance in this regard. For efficient conductivity in photovoltaic cells to occur, charge separation of the excitons that form upon photoirradiation is necessary.[5] It is known that the existence of intramolecular heterojunctions facilitates this separation.[6,7] Such heterojunctions can be achieved by the inclusion of both electron-donating and -accepting components in the same molecule,[8,9] which causes the spatial separation of the highest occupied and lowest unoccupied molecular orbitals (HOMO and LUMO), thus aiding charge separation of the excition.

It is therefore of interest to examine the excited-state properties of oligothiophenes and, in particular, oligothiophenes that have been substituted with groups possessing a strong electronic influence. The steady-state[10] and transient[11−13] absorption and emission spectra of all the soluble unsubstituted oligothiophenes have been reported in various solvents. A number of trends have been observed upon increasing oligothiophene size, in particular, there is an increase in the fluorescence quantum yield and lifetime accompanied by a concomitant decrease in the triplet quantum yield.[14]

In this paper the emission properties of several styryl-substituted terthiophenes, R-*pet*, have been investigated and compared to those of unsubstituted terthiophene (3T). The structures of the examined compounds are shown in Figure 1. Picosecond time-resolved and solvent-dependent steady-state fluorescence studies have been performed in conjunction with density functional theory (DFT) calculations to improve the understanding of the R-*pet* excited-state structures. Alteration of the electronic nature of the para group on the phenyl ring from inert −H to the strongly electron donating $-NMe_2$ causes significant modifications to the excited-state properties, with a change in the excited-state character from a π,π^* to a charge-transfer state.

Experimental Section

The synthesis and purification methods of the styryl-substituted terthiophenes studied are described elsewhere.[15] Unsubstituted terthiophene was purchased from Aldrich and used without further purification. The solvents (Aldrich, spec-

* Corresponding author. Fax: (+64) 3 479 7906. E-mail: kgordon@chemistry.otago.ac.nz.
[†] University of Otago.
[‡] The University of Hong Kong.
[§] Massey University.

10.1021/jp0600312 CCC: $33.50
Published on Web 05/26/2006

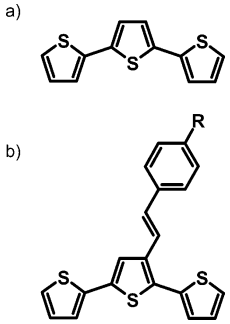

Figure 1. Chemical structures of the compounds studied here: unsubstituted terthiophene, 3T (a), and R-*pet*, where *pet* refers to phenyl ethenyl terthiophene and R = $-NMe_2$, $-NH_2$, $-OMe$, $-H$, $-CN$ and $-NO_2$.

trophotometric grade) considered here are cyclohexane (C_6H_{12}), chloroform ($CHCl_3$), dichloromethane (CH_2Cl_2) and acetonitrile (CH_3CN), in order of increasing dielectric constant and polarity.

Electronic absorption spectra were measured of $10^{-6}-10^{-7}$ mol L^{-1} solutions in C_6H_{12}, $CHCl_3$, CH_2Cl_2 and CH_3CN for all compounds at room temperature from 200 to 800 nm on a Varian Cary 500 Scan UV−vis−NIR spectrophotometer using Cary WinUV Scan Application software.

Steady-state fluorescence spectra were measured of the same $10^{-6}-10^{-7}$ mol L^{-1} solutions used in the absorption measurements. A Perkin-Elmer Luminescence Spectrometer LS50B with FL Winlab v. 4.00.02 software was used over the range 300−800 nm. Various excitation wavelengths over 300−400 nm were trialed for each compound. Each fluorescence spectrum was corrected using a quinine sulfate spectrum provided by Dr. R. A. Velapoldi. Fluorescence quantum yields, ϕ_F, were measured for the C_6H_{12}, $CHCl_3$ and CH_3CN solutions using 1×10^{-7} mol L^{-1} quinine sulfate in 0.1 mol L^{-1} H_2SO_4 as the standard ($\phi_F = 0.546$).[16]

Picosecond time-resolved fluorescence (TRF) spectra were measured using a system previously described[17] for the compounds 3T, NMe_2-*pet*, NH_2-*pet*, MeO-*pet* and CN-*pet* in 5×10^{-4} mol L^{-1} acetonitrile solutions. Briefly, the Kerr gated time-resolved emission measurements were done using a Ti:sapphire regenerative amplified laser operated at 1 mJ/pulse, 150 fs, 1 kHz and 800 nm and its 400 nm frequency doubled output. The 320 nm excitation pulses were made by mixing the 800 nm pulses and the 533 nm output from a home-built OPA system pumped by the 400 nm laser pulses. The excitation pulses (about 1 μJ) were lightly focused (about 100 μm diameter) onto a 0.5 mm thickness liquid stream of sample placed at one focus of an elliptical mirror. The elliptical mirror collected the emission from the sample and imaged the collected light through a film polarizer. The collected light was then focused into the Kerr medium (a 2 mm UV cell with benzene in it) at the other focus point of the ellipse. The Kerr medium for the experiments was located between a crossed pair of polarizers with an extinction ratio of about 10^4. The Kerr gating pulse (800 nm) was polarized at 45° and focused into the Kerr medium with an adjusted intensity so as to create a "half-waveplate" that rotates the polarization of emission from the sample. This allows some of the emitted light to be transitted through the Glan Taylor polarizer for the duration of the induced anisotropy produced by the femtosecond gating pulse. Then the emission that passed through the second polarizer was focused into a monochromator and detected by a liquid nitrogen cooled CCD detector. All of the time-resolved fluorescence spectra were found by subtracting the negative time delay signal from the positive time delay signal and the instrument response was approximately 1 ps. The magic angle configuration was employed to eliminate the effect of sample reorientation on the time-resolved emission. A computer controlled optical delay line was used to set the different time-delays employed in the Kerr gated time-resolved fluorescence experiments. The time zero delay between the pump and probe laser beams in the Kerr gated experiments were determined by employing fluorescence depletion of *trans*-stilbene. The time zero was detemined by varying the optical delay between the pump and probe beams to a position where the depletion of the stilbene fluorescence was halfway to the maximum fluorescence depletion by the probe laser and the accuracy of the time zero measurement was estimated to be ±0.3 ps. The fluorescence depletion of *trans*-stilbene was also used to obtain a typical cross correlation time between the pump and probe pulses and was found to be about 1 ps (fwhm).

Results and Discussion

1. Steady-State Emission Spectroscopy. The absorption, emission and Stokes shift data for 3T and R-*pet* in the various solvents are presented in Table 1. The photophysical parameters of 3T have been previously investigated in a variety of solvents and it has been found that solvent has little influence on the emission properties,[10,14] a result reproduced here. The 3T absorption spectrum contains one broad unstructured band with a maximum at ~352 nm, and the emission spectrum possesses a band maximum at ~430 nm and a shoulder at ~410 nm. The more structured appearance of the emission spectrum suggests that the excited state is more planar and rigid than the ground state.[18] This is believed to be a result of the quinoidization of the thiophene backbone upon creation of the excited state. The increased double bond character of the inter-ring bonds thus leads to the planarization of the molecule upon excitation.[19]

Introduction of the styryl group, to create H-*pet*, causes significant changes to the absorption and emission spectra (Figure 2). The absorption maximum now lies at ~312 nm, the result of the new styryl-based molecular orbitals HOMO−1 and LUMO+1,[20] whereas the prominent 350 nm shoulder is at approximately the same wavelength as the original 3T absorption maximum. This shoulder is assigned to the HOMO → LUMO transition, the two orbitals being localized primarily on the terthiophene backbone. The calculated spatial distribution and relative energies of the HOMO and LUMO are unperturbed by styryl substitution and this is consistent with the observation of an unshifted absorption band with respect to 3T. The HOMO, as calculated by DFT theory[20] and seen in other polyenic systems,[21] has the same phase across the terthiophene CC double bonds whereas the LUMO has the same phase across the single bonds. Thus the S_1 state of H-*pet* (and 3T) is predicted to possess π,π^* character. The H-*pet* fluorescence spectrum is broad and featureless with a maximum at ~455 nm in all solvents except cyclohexane, where the maximum is slightly blue-shifted to 447 nm and a shoulder is apparent at 436 nm. H-*pet* therefore has only modest solvatochromic behavior that may be quantified by a determination of the relative Stokes shifts in the various solvents.

The Stokes shift is determined as the difference in wavenumber between the lowest energy absorption (a shoulder in all of the spectra and thus subject to uncertainty) and the highest energy florescence band (a shoulder in the case of some of the spectra). The way in which the Stokes shift alters with solvent reveals information about the emitting excited state.[22] One way to gain some insight into the nature of the emitting exciting state is to determine the *change in dipole moment* on going

TABLE 1: Absorption, Fluorescence, and Stokes Shift Data for Each Compound in Each Solvent

	cyclohexane			chloroform			dichloromethane			acetonitrile			
	abs[a]/ nm	em[a]/ nm	Stokes shift[b]/ cm^{-1}	abs/ nm	em/ nm	Stokes shift/ cm^{-1}	abs/ nm	em/ nm	Stokes shift/ cm^{-1}	abs/ nm	em/ nm	Stokes shift/ cm^{-1}	$\Delta\mu$/D[c]
3T		427			432			431			427		
	350	410	4200	355	415	4100	354	413	4000	352	408	3900	0
H-*pet*	308	448		312			312			310			
	349	436	5700	350	453	6500	350	455	6600	350	456	6600	7.9
MeO-*pet*	318	445		324	451		324	451		322	449		
	362	425	4100	363	435	4600	363	436	4600	358	433	4800	6.7
NH_2-*pet*	328	449		333			336			337			
	366	428	4000	370	458	5200	368	468	5800	370	510	7400	14.7
CN-*pet*	318	470		324			322			320			
	356	456	6200	358	495	7700	359	501	7900	353	508	8600	12.5
NMe_2-*pet*	345	460		350			351			350			
	372	440	4200	383	478	5200	382	504	6300	377	544	8100	16.0
NO_2-*pet*	335	497		345			345			342			
	385	474	4900	405			401			395			

[a] ±1 nm. [b] ±200 cm^{-1}. [c] Calculated from Lippert−Mataga plot.

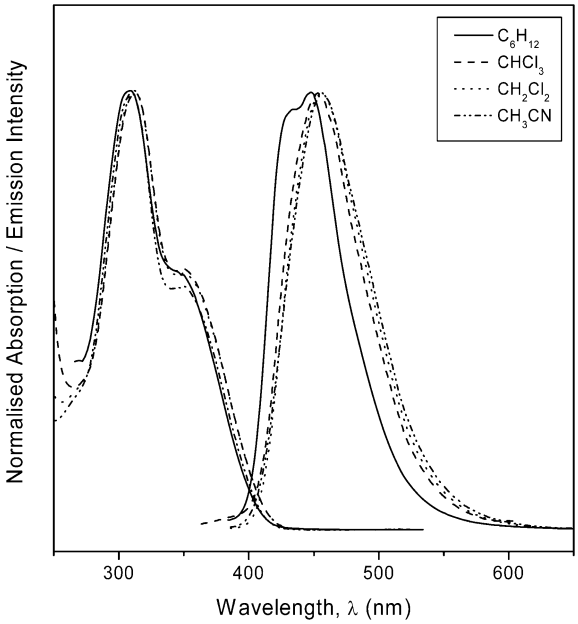

Figure 2. Normalized absorption (250−400 nm) and emission (400−600 nm) spectra of H-*pet* in cyclohexane (C_6H_{12}), chloroform ($CHCl_3$), dichloromethane (CH_2Cl_2) and acetonitrile (CH_3CN).

from the ground (μ_g) to excited state (μ_e). Estimates of these values may be obtained experimentally using the Lippert−Mataga equation (1). This relates the Stokes shift (ν_{st}, cm^{-1})

$$\nu_{st} = \frac{2(\mu_e - \mu_g)^2}{4\pi\epsilon_0}\frac{\Delta f}{hca^3} + C \qquad (1)$$

with the solvent polarity parameter (Δf), the Onsager radius of the fluorophores of interest (a, m) and the fundamental constants (h, J s; ϵ_0, J^{-1} C^2 m^{-1}; and c, cm s^{-1}).

For the Onsager radius, we have used the value of 6.2 Å, which is half of the long axis of the 3T and R-*pet* molecules. This value was determined by examining the calculated structures of the compounds of interest.[20] The solvent polarity parameter (Δf) is calculated from the dielectric constant (ϵ) and refractive index (n) of the solvent of interest, as shown in eq 2.

$$\Delta f = \left(\frac{\epsilon - 1}{2\epsilon + 1}\right) - \left(\frac{n^2 - 1}{2n^2 + 1}\right) \qquad (2)$$

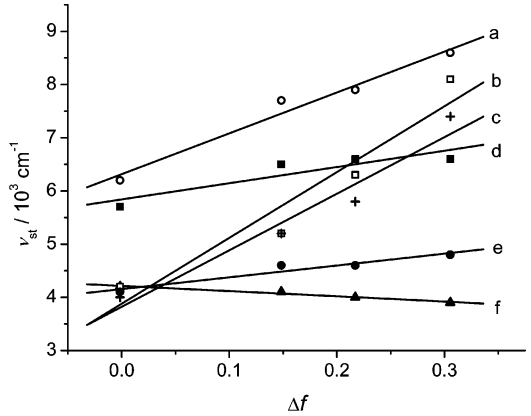

Figure 3. Lippert−Mataga plots: (a) CN-*pet* (○); (b) NMe_2-*pet* (□); (c) NH_2-*pet* (+); (d) H-*pet* (■); (e) MeO-*pet* (●); 3T (▲). Solid lines are lines of fit for each data set.

The Lippert−Mataga plots are shown in Figure 3; gradient values range from −980 cm^{-1} for 3T to 12 500 cm^{-1} for NMe_2-*pet*.[23] The plots appear linear having $R^2 > 0.9$. This observed linearity suggests that the large solvent-dependent shifts in the fluorescence spectrum are a consequence of the dipole−dipole interactions between solvent and solute.[24,25] The values for the change in dipole ($\Delta\mu = \mu_e - \mu_g$) calculated from (1) and (2) are shown in Table 1.

The compounds studied fall into two categories in their Lippert−Mataga plot behavior; the 3T, H-*pet* and MeO-*pet* have much shallower gradients (−980, +3000, and +2200 cm^{-1}, respectively, Figure 3) than NH_2-*pet*, CN-*pet* and NMe2-*pet* (+10 600, +7700, and +12 500 cm^{-1} respectively). The S_1 state of 3T has previously been assigned as a π,π^* state[10] and given the close similarities between the HOMO and LUMO of 3T and H-*pet* and their smaller calculated $\Delta\mu$ values, it seems reasonable that the S_1 state of H-*pet* is also of π,π^* character. The calculated HOMO and LUMO of MeO-*pet* (Figure 4a,b) show that both orbitals are almost fully delocalized over both styryl and terthiophene moieties (although the LUMO does have less density on the phenyl ring), implying that the HOMO → LUMO transition would also possess π,π^* character.

The substitution of groups in the para position of the phenyl ring with stronger electron donating or accepting character causes appreciable solvent dependence in the optical properties of the compounds.[26] This is evident most clearly in the NMe_2-*pet* emission spectra (Figure 5). The absorption maximum of this compound is at 345−349 nm, and the emission maximum

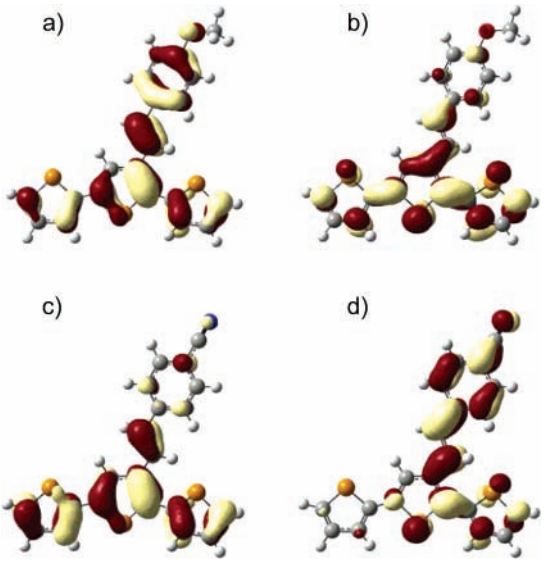

Figure 4. Calculated (B3LYP/6-31G(d)) HOMO (a) and LUMO (b) of MeO-*pet* and the HOMO (c) and LUMO (d) of CN-*pet*.

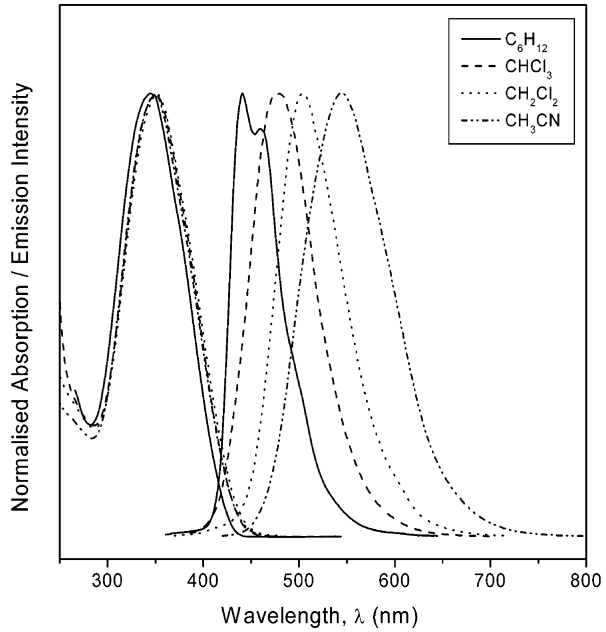

Figure 5. Normalized absorption (250−450 nm) and emission (400−700 nm) spectra of NMe_2-*pet* in cyclohexane (C_6H_{12}), chloroform ($CHCl_3$), dichloromethane (CH_2Cl_2) and acetonitrile (CH_3CN).

ranges from 440 nm (in cyclohexane) to 554 nm (in acetonitrile). As with the previous compounds, cyclohexane provides a more structured fluorescence spectrum and the emission maximum is accompanied by another peak at 460 nm. The slope of the Lippert−Mataga plot for NMe_2-*pet* is 4 times that of H-*pet*. The considerable solvent sensitivity observed in the fluorescence spectra of NMe_2-*pet* arises due to the nature of the emitting state.[26] The state created by the HOMO → LUMO transition, the S_1 state, has intramolecular charge-transfer character because the HOMO of this molecule is localized primarily on the styryl substituent whereas the LUMO is located on the terthiophene backbone.[20] This prediction is supported by the solvent dependence observed in the emission spectra. Due to the transfer of electron density from the styryl to the terthiophene moiety upon excitation, a dipole is created in the excited state, much larger than that possessed by the ground state. Acetonitrile is a polar solvent and therefore able to stabilize this polarized excited state

TABLE 2: Fluorescence Quantum Yields, ϕ_F, of Each Compound in Cyclohexane (C_6H_{12}), Chloroform ($CHCl_3$), and Acetonitrile (CH_3CN), Calculated Using Corrected Fluorescence Spectra and Quinine Sulfate in H_2SO_4 as the Standard

	C_6H_{12}	$CHCl_3$	CH_3CN
3T	0.051	0.049	0.052
H-*pet*	0.047	0.042	0.048
MeO-*pet*	0.054	0.048	0.037
NH_2-*pet*	0.061	0.037	0.022
CN-*pet*	0.074	0.026	0.013
NMe_2-*pet*	0.160	0.052	0.028
NO_2-*pet*	0.018	-	-

by the reorientation of the solvent molecules to accommodate the increased dipole, lowering the energy of the system.[22] This phenomenon of solvent relaxation and the accompanying increase in Stokes shift with increasing solvent polarity are well-known in CT compounds.[26,27]

The fluorescence spectra of CN-*pet* and NH_2-*pet* are also strongly solvent dependent and large dipole moment changes are calculated for these compounds. In the case of CN-*pet*, where the −CN group is an electron acceptor, the HOMO is localized on the terthiophene and the LUMO on the styryl substituent, as shown in Figure 4c,d.

In summary, the solvatochromic behavior of these compounds may be rationalized within the framework of the Lippert−Mataga model. Analysis using this model reveals that for those compounds that possess a spatially separated HOMO and LUMO, large dipole moment changes upon photoexcitation are determined from the experimental data. Interestingly, both CN-*pet* and NH_2-*pet* show appreciable $\Delta\mu$ (12.5 and 14.7 D, respecitvely) despite the fact that their substituent groups have opposing inductive effects. In the case of CN-*pet* the HOMO is localized on the terthiophene backbone and the LUMO on the styryl substituent; for NH_2-*pet* the converse is true. Thus it is the spatial separation of the frontier MOs that is the key to the existence of a charge-transfer state rather than a specific direction of the electronic transition.

The fluorescence quantum yield, ϕ_F, of each compound has been calculated for each solvent using quinine sulfate as the standard (Table 2).[16] For 3T and H-*pet*, the quantum yield remains the same across the three solvents trialed (acetonitrile, chloroform and cyclohexane). The value of $\phi_F = 0.052$ for 3T, measured in acetonitrile, is close to that previously reported ($\phi_F = 0.056$).[14] The absence of change in the quantum yield with solvent in these two compounds is consistent with the lack of solvent dependence observed in the emission spectra. MeO-*pet* shows a very small increase in quantum yield with decreasing solvent polarity, from $\phi_F = 0.037$ in acetonitrile to $\phi_F = 0.054$ in cyclohexane.

However, for those molecules with more pronounced CT characteristics and a strong solvent dependence in the emission maxima, the increase in ϕ_F with decreasing polarity of the solvent becomes appreciably more marked. For example, the fluorescence quantum yield of NMe_2-*pet* in acetonitrile is 0.028 but this increases to 0.16 in cyclohexane. NO_2-*pet*, which is virtually nonfluorescent in acetonitrile, has a measurable quantum yield of 0.018 in cyclohexane. It is known that aromatic molecules containing $-NO_2$ groups have only weak emission due to efficient nonradiative processes.[22] The rise in quantum yield from acetonitrile to cyclohexane is consistent with the previous result of increasing Stokes shift with solvent polarity. The larger Stokes shift provided by polar solvents such as acetonitrile indicates a greater change in the molecular geometry from the ground (S_0) to the excited (S_1) state and therefore a

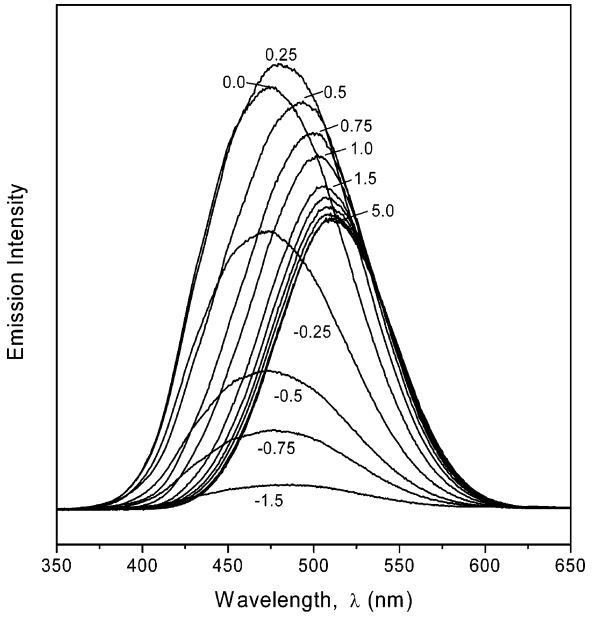

Figure 6. Picosecond time-resolved fluorescence spectra of NH_2-*pet* (5×10^{-4} M) in acetonitrile at various delay times (ps).

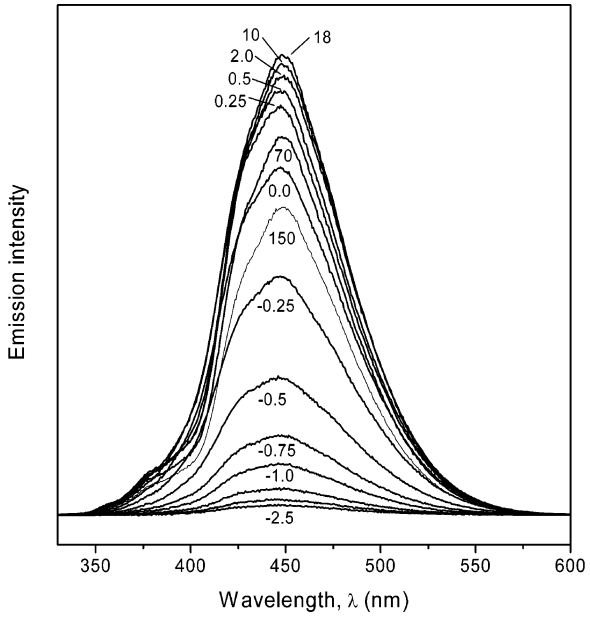

Figure 7. Picosecond time-resolved fluorescence spectra of MeO-*pet* (5×10^{-4} M) in acetonitrile at various delay times (ps).

greater displacement of the S_1 potential energy surface relative to the S_0 surface. This would cause a larger overlap between the wave functions of the relaxed S_1 state and the higher vibrational levels of the S_0 state, leading to more efficient nonradiative processes and therefore lowering the quantum yield. This statement relies upon the assumption that $k_{nr} > k_r$, which is common in organic species.[28] Conversely, nonpolar cyclohexane is associated with a significantly smaller Stokes shift; thus the pertinent wave functions will have only a small overlap, reducing the nonradiative rate constant and increasing the quantum yield of fluorescence.[29]

2. Picosecond Time-Resolved Fluorescence Spectroscopy. The picosecond time-resolved fluorescence (TRF) spectra of some styryl terthiophenes have also been measured in acetonitrile. The three compounds exhibiting charge-transfer characteristics in the steady-state emission spectra (NMe_2-*pet*, NH_2-*pet* and CN-*pet*) do so in their TRF spectra as well. At very early delay times, −5 to +0.25 ps, the emission maximum is blue-shifted relative to the corresponding steady-state maximum. At 0.25 ps, for example, NH_2-*pet* has its emission maximum at 473 nm (the TRF spectra have not been calibrated for wavelength sensitivity, so the data indicate the relative profile change with time delay but not the absolute position of the emission maximum), as shown in Figure 6. As the delay increases toward 5 ps, the emission red shifts toward 510 nm, where it remains at this steady value for delay times of 5−6000 ps. The corresponding red shifts observed for NMe_2-*pet* and CN-*pet* are 37 and 19 nm, respectively. In contrast, 3T and MeO-*pet*, compounds that possess a π,π^* S_1 state rather than a CT S_1 state, do not show this red shift and the emission maximum remains constant over the entire time range (Figure 7). The red shift is a manifestation of the greater extent of solvent relaxation that is required for the CT molecules,[22] a process that occurs on the early picosecond time scale and lowers the energy of the charge-separated S_1 state. The fluorescence spectra measured at very early delay times therefore represent emission prior to solvent relaxation.

The lifetime of the S_1 state for each molecule in acetonitrile was calculated by measuring the decay of the emission maximum with time. In each case the fluorescence decay can be fitted to a first-order exponential curve. Some examples are displayed in Figure 8. The lifetime, τ, of the 3T S_1 state is 140 ps, a value very close to those previously measured in other solvents.[14,30−32] The lifetimes of the styryl terthiophenes are significantly longer than this. CN-*pet* and MeO-*pet* have similar S_1 lifetimes (320 and 360 ps, respectively) whereas NMe_2-*pet* has the longest singlet lifetime of 670 ps. Unsubstituted terthiophene, 3T, is known to undergo efficient intersystem crossing (ISC), forming the triplet state in high quantum yield.[13,33] This is due to the S_1 and T_2 states being almost isoenergetic[34] and has been deemed the reason for the short S_1 lifetime. For longer oligothiophenes, the rate of ISC decreases because of the increase in the energy difference between the S_1 and T_2 states,[13] and consequently the fluorescence lifetime increases. It is therefore probable that the styryl terthiophenes, which have an effective conjugation length of the equivalent

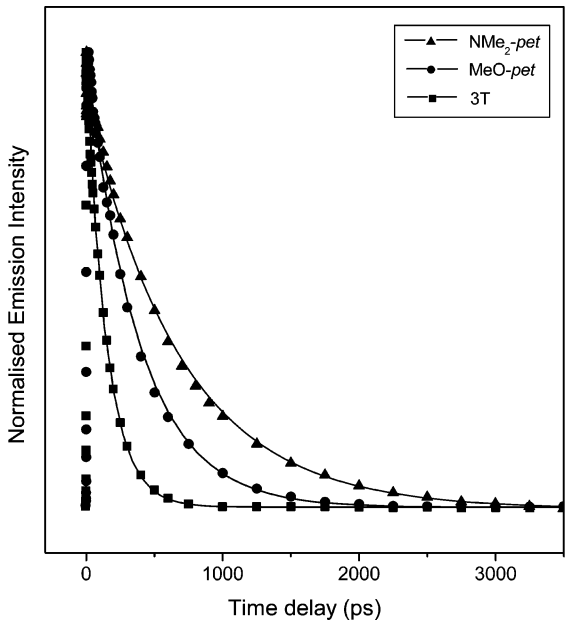

Figure 8. Decay of the fluorescence intensity of NMe_2-*pet* (▲), MeO-*pet* (●) and 3T (■) in acetonitrile measured at the emission maximum (steady-state wavelength), fitted to first-order exponential curves.

TABLE 3: Photophysical Properties of Each Compound in Acetonitrile

	τ/ps[a]	$10^{-7}k_r/s^{-1}$	$10^{-9}k_{nr}/\ s^{-1}$	k_{nr}/k_r
3T	140	37	6.8	18
MeO-*pet*	360	10	2.7	26
CN-*pet*	320	4.1	3.1	76
NH_2-*pet*	410	5.9	2.4	41
NMe_2-*pet*	670	4.2	1.5	35

[a] The lifetimes have been calculated from the decay of the emission maximum (steady-state wavelength).

of five thiophene rings,[20] have longer S_1 lifetimes than 3T because of a decrease in the rate of ISC.

For some compounds, the fluorescence decay is dependent upon the wavelength at which the decay is examined. In the case of CN-*pet*, NH_2-*pet*, and NMe_2-*pet*, the intensity decay on the blue side of the emission band is more rapid than on the red side, producing an increase in fluorescence lifetime with increasing wavelength. This situation generally arises if the rate of solvent relaxation is comparable to the rate of fluorescence decay.[22] Consequently, emission on the blue side of the band is affected by fluorescence decay from both the Franck−Condon and relaxed states whereas emission on the red side is solely due to emission after solvent relaxation. This can occur as a result of numerous factors, including general solvent effects or the formation of charge-transfer states.

Possessing both quantum yield and fluorescence lifetime data for these compounds allows the calculation of other photophysical parameters, namely the radiative rate constant k_r ($k_r = \phi_F/\tau_F$, assuming that phosphorescence is negligible, a reasonable assumption for terthiophenes[14,34]) and the nonradiative rate constant k_{nr} ($k_{nr} = \tau^{-1} - k_r$). These results are shown in Table 3. As expected, 3T has the highest k_{nr} value (which includes k_{ISC}) but due to its combination of lowest τ and highest ϕ it also has the highest k_r value. It is therefore more useful to consider the ratio k_{nr}/k_r. It is apparent that the three CT compounds, NMe_2-*pet*, NH_2-*pet* and CN-*pet* have the highest ratio ($k_{nr}/k_r = 35-76$) whereas 3T has the lowest ($k_{nr}/k_r = 18$) and MeO-*pet* is intermediate ($k_{nr}/k_r = 26$). This higher proportion of k_{nr} observed for the CT compounds is consistent with their larger Stokes shifts in acetonitrile and the theory that these molecules have undergone a larger geometry change in the excited state in acetonitrile, thereby displacing the S_1 potential energy surface, creating a greater S_0/S_1 wave function overlap and increasing the efficiency of nonradiative decay. Indeed, CN-*pet* has both the largest Stokes shift in acetonitrile and the highest k_{nr}/k_r ratio whereas 3T has the lowest of both values and MeO-*pet* the second lowest. MeO-*pet* has the highest k_r of all the styryl terthiophenes and this can also be linked to the smaller Stokes shift observed for this molecule and therefore smaller geometry change upon excitation. This point also supports the suggestion that the MeO-*pet* S_1 state is of π,π^* character rather than CT character, which produces smaller k_r values and higher k_{nr}/k_r ratios.

Conclusions

A combination of steady-state and picosecond time-resolved fluorescence spectroscopy has shown that within a series of styryl-substituted terthiophenes, two distinct types of S_1 state are possible. Those compounds possessing a strongly electron donating or accepting R group in the para position of the phenyl ring, such as NMe_2-*pet*, NH_2-*pet* and CN-*pet*, show evidence of a charge-transfer S_1 state, as evidenced by their Lippert−Mataga plots. This is indicated by the appreciable solvatochromism in the emission spectra, the increase in fluorescence quantum yield with decreasing solvent polarity and the red shifting observed at very early delay times in the ps-TRF spectra for these three compounds. In addition, density functional theory calculations have suggested that the HOMO and LUMO are spatially separated, supporting the assignment of a charge-transfer S_1 state. In contrast, H-*pet*, MeO-*pet* and 3T show little to no trends with solvent polarity and the delocalized nature of both the HOMO and LUMO indicate the presence of a π,π^* S_1 state. By judicious choice of the para R group in styryl terthiophenes, therefore, it is possible to tune the nature of the first excited singlet state from π,π^* to a charge-transfer character. Charge-transfer states may offer possible strategies for solar cells in which charge separation is a key step.

Acknowledgment. The authors are grateful to the New Zealand Foundation of Science, Research and Technology and the University of Otago for support. D.L.P. acknowledges partial support from a grant from the Research Grants Council of Hong Kong (HKU 1/01C and HKU-7021/03P).

References and Notes

(1) Pron, A.; Rannou, P. *Prog. Polym. Sci.* **2001**, *27*, 135.
(2) Dai, L.; Winkler, B.; Dong, L.; Tong, L.; Mau, A. W. H. *Adv. Mater.* **2001**, *13*, 915.
(3) Horowitz, G. *Adv. Mater.* **1998**, *10*, 365.
(4) Wallace, G. G.; Dastoor, P. C.; Officer, D. L.; Too, C. O. *Chem. Innovation* **2000**, *30*, 14.
(5) Gazotti, W. A.; Nogueira, A. F.; Girotto, E. M.; Micaroni, L.; Martini, M.; das Neves, S.; De Paoli, M. A. *Handbook of Advanced Electronic and Photonic Materials and Devices* **2001**, *10*, 53.
(6) Zhang, F.; Svensson, M.; Andersson, M. R.; Maggini, M.; Bucella, S.; Menna, E.; Inganas, O. *Adv. Mater.* **2001**, *13*, 1871.
(7) Cravino, A.; Zerza, G.; Neugebauer, H.; Maggini, M.; Bucella, S.; Menna, E.; Svensson, M.; Andersson, M. R.; Brabec, C. J.; Sariciftci, N. S. *J. Phys. Chem. B* **2002**, *106*, 70.
(8) Fujitsuka, M.; Masuhara, A.; Kasai, H.; Oikawa, H.; Nakanishi, H.; Ito, O.; Yamashiro, T.; Aso, Y.; Otsubo, T. *J. Phys. Chem. B* **2001**, *105*, 9930.
(9) Van Hal, P. A.; Knol, J.; Langeveld-Voss, B. M. W.; Meskers, S. C. J.; Hummelen, J. C.; Janssen, R. A. J. *J. Phys. Chem. A* **2000**, *104*, 5974.
(10) Becker, R. S.; de Melo, S.; Macanita, A. L.; Elisei, F. *Pure Appl. Chem.* **1995**, *67*, 9.
(11) Rentsch, S.; Chosrovian, H.; Grebner, D.; Naarmaan, H. *Synth. Met.* **1993**, *57*, 4740.
(12) Chosrovian, H.; Rentsch, S.; Grebner, D.; Dahm, D. U.; Birckner, E.; Naarmann, H. *Synth. Met.* **1993**, *60*, 23.
(13) Paa, W.; Yang, J. P.; Rentsch, S. *Appl. Phys. B* **2000**, *71*, 443.
(14) Becker, R. S.; de Melo, J. S.; Macanita, A. L.; Elisei, F. *J. Phys. Chem.* **1996**, *100*, 18683.
(15) Collis, G. E.; Burrell, A. K.; Scott, S. M.; Officer, D. L. *J. Org. Chem.* **2003**, *68*, 8974.
(16) Sierra, C. A.; Lahti, P. M. *Chem. Mater.* **2004**, *16*, 55.
(17) Ma, C.; Kwok, W. M.; Chan, W. S.; Zuo, P.; Kan, J. T. W.; Toy, P. H.; Phillips, D. L. *J. Am. Chem. Soc.* **2005**, *127*, 1463.
(18) Tirapattur, S.; Belletete, M.; Drolet, N.; Leclerc, M.; Durocher, G. *Macromolecules* **2002**, *35*, 8889.
(19) Clarke, T. M.; Gordon, K. C.; Officer, D. L.; Grant, D. K. *J. Phys. Chem. A* **2005**, *109*, 1961.
(20) Clarke, T. M.; Gordon, K. C.; Officer, D. L.; Hall, S. B.; Collis, G. E.; Burrell, A. K. *J. Phys. Chem. A* **2003**, *107*, 11505.
(21) Casado, J.; Miller, L. L.; Mann, K. R.; Pappenfus, T. M.; Kanemitsu, Y.; Orti, E.; Viruela, P. M.; Pou-Amerigo, R.; Hernandez, V.; Lopez Navarrete, J. T. *J. Phys. Chem. B* **2002**, *106*, 3872.
(22) Lakowicz, J. R. *Principles of fluorescence spectroscopy*; Kluwer Academic/Plenum: New York, 1999.
(23) The uncertainties in these plots are of the order of ± 1000 cm^{-1}.
(24) Reichardt, C. *Chem. Rev.* **1994**, *94*, 2319.
(25) Kamlet, M. J.; Abboud, J. L.; Taft, R. W. *J. Am. Chem. Soc.* **1977**, *99*, 6027.
(26) Maus, M.; Rettig, W.; Bonafoux, D.; Lapouyade, R. *J. Phys. Chem. A* **1999**, *103*, 3388.
(27) Dey, J.; Warner, I. M. *J. Photochem. Photobiol., A* **1998**, *116*, 27.
(28) Turro, N. J. *Modern Molecular Photochemistry*; Benjamin/Cummings Publishing Co.: Menlo Park, CA, 1978.

(29) This simple interpretation does not include how the solvent may affect the structural changes observed; these provide an additional contribution to the observed Stokes shifts, particularly for charge-transfer states.

(30) Colditz, R.; Grebner, D.; Helbig, M.; Rentsch, S. *Chem. Phys.* **1995**, *201*, 309.

(31) Grebner, D.; Helbig, M.; Rentsch, S. *J. Phys. Chem.* **1995**, *99*, 16991.

(32) Helbig, M.; Hein, J.; Rentsch, S.; Burger, H.; Hobert, H. *Chem. Phys.* **1998**, *227*, 111.

(33) Paa, W.; Yang, J.-P.; Helbig, M.; Hein, J.; Rentsch, S. *Chem. Phys. Lett.* **1998**, *292*, 607.

(34) Rentsch, S.; Yang, J. P.; Paa, W.; Birckner, E.; Schiedt, J.; Weinkauf, R. *Phys. Chem. Chem. Phys.* **1999**, *1*, 1707.